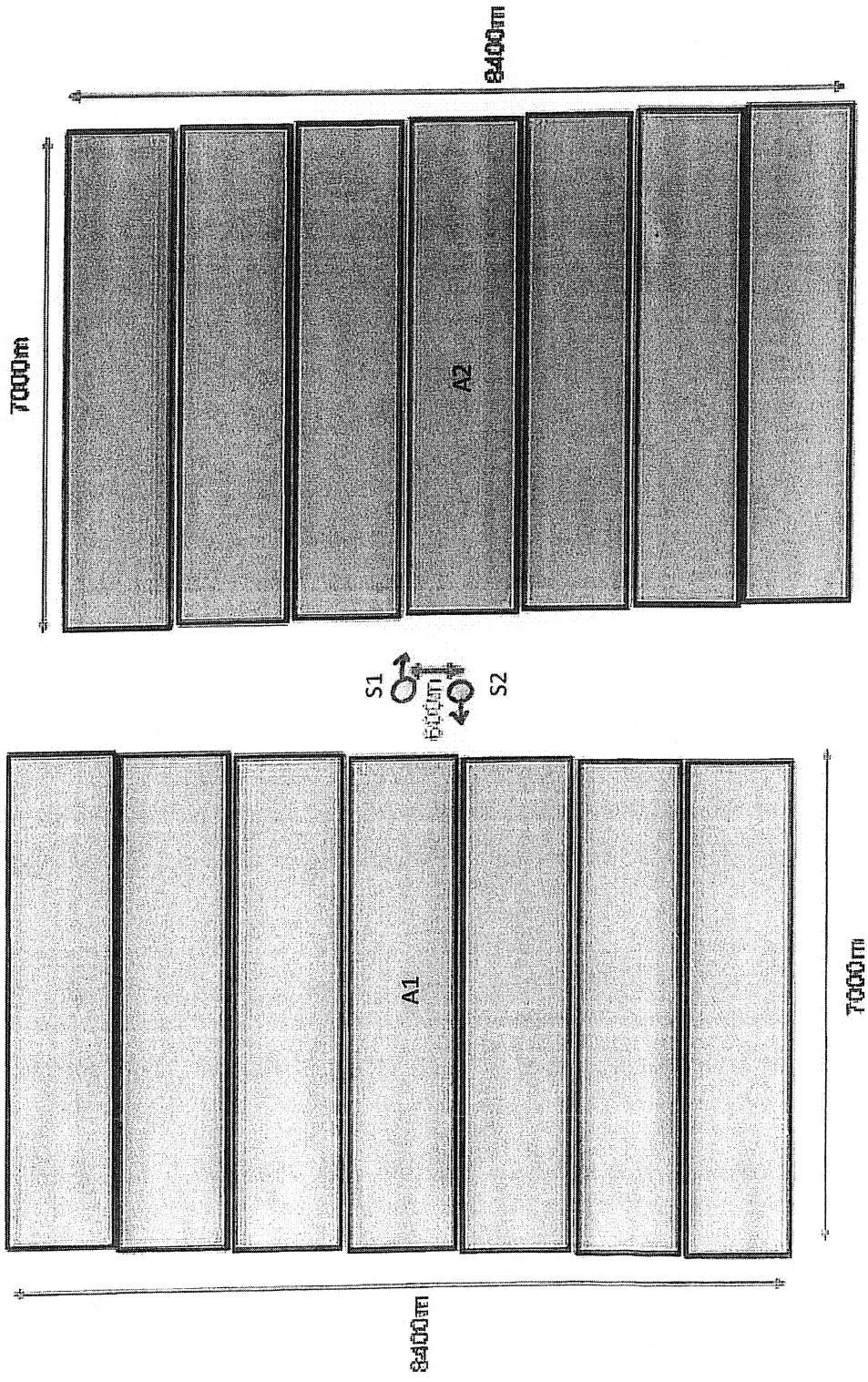


FIG. 1

Image (subsurface offset) gathers from using cross correlation imaging condition :

$$\text{Image}_{ss\_offset}(\vec{x},\vec{h}) = \sum_{\omega} U(\vec{x},\omega,\vec{x}+\vec{h}) * D^{*}(\vec{x},\omega,\vec{x}-\vec{h}) \qquad (1.1)$$

$$\text{Image}_{ss\_offset}(\vec{x},\vec{h}) = \sum_{t} U(\vec{x},t,\vec{x}+\vec{h}) * D(\vec{x},t,\vec{x}-\vec{h}) \qquad (1.2)$$

Image (subsurface offset) gathers from using deconvolution imaging condition :

$$\text{Image}_{ss\_offset}(\vec{x},\vec{h}) = \sum_{\omega} \frac{U(\vec{x},\omega,\vec{x}+\vec{h}) * D^{*}(\vec{x},\omega,\vec{x}-\vec{h})}{D(\vec{x},\omega,\vec{x}-\vec{h}) * D^{*}(\vec{x},\omega,\vec{x}-\vec{h})} \qquad (1.3)$$

Image gathers from subsurface offset domain to angle domain :

$$\text{Image}_{ss\_offset}(\vec{x},\vec{h}) \quad \underrightarrow{\text{subsurface offset to angle}} \quad \text{Image}_{angle}(\vec{x},\phi,\varphi) \qquad (2)$$

$\vec{x} = (x, y, z)$ is the subsurface coordinate

$\vec{h} = (h_x, h_y, h_z)$ is the half source-receiver offset for generating image gathers

FIG. 2

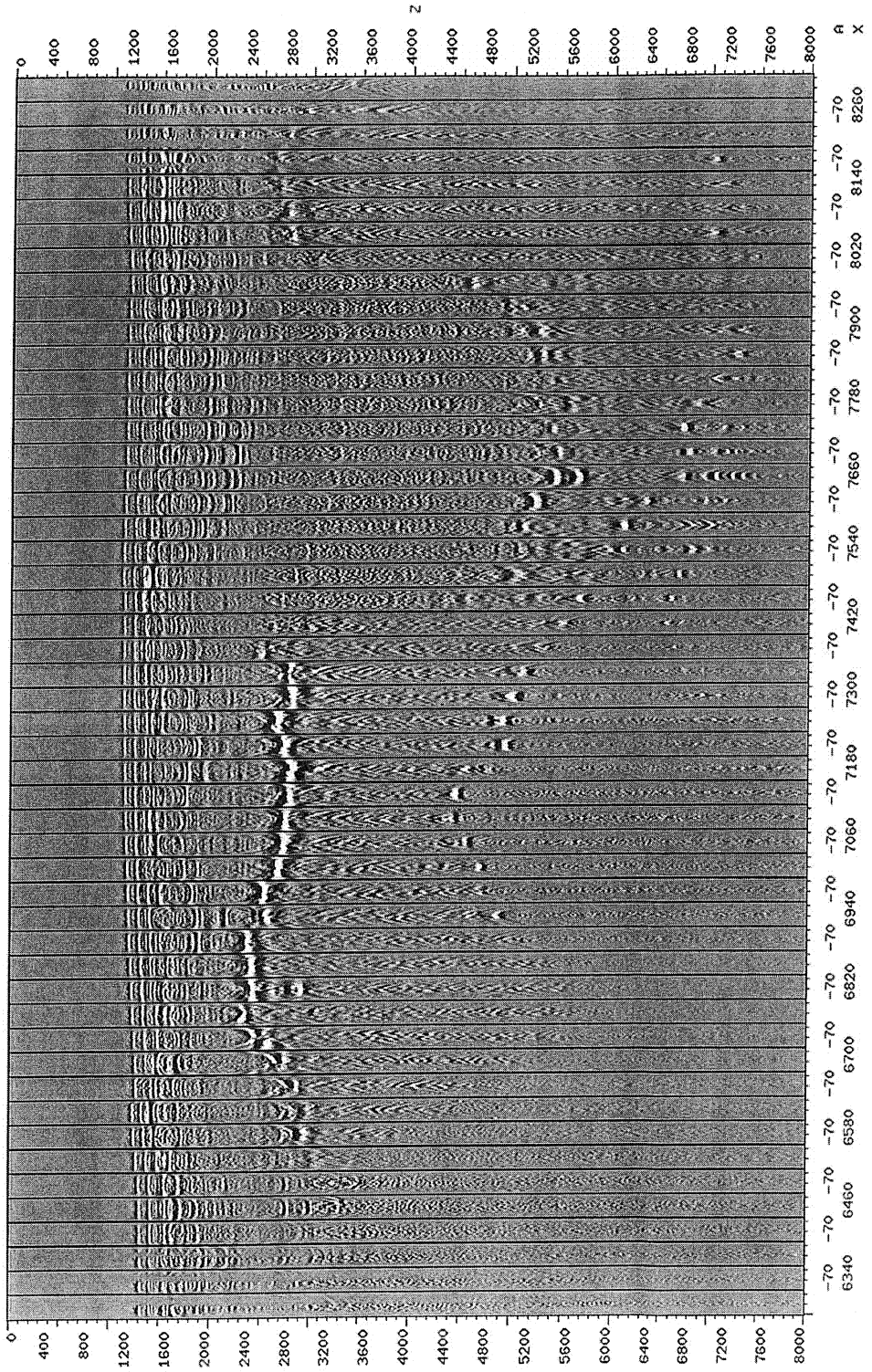

Z
X
0
400
800
1200
1600
2000
2400
2800
3200
3600
4000
4400
4800
5200
5600
6000
6400
6800
7200
7600
8000
-70
6340
6460
6580
6700
6820
6940
7060
7180
7300
7420
7540
7660
7780
7900
8020
8140
8260

FIG. 3A

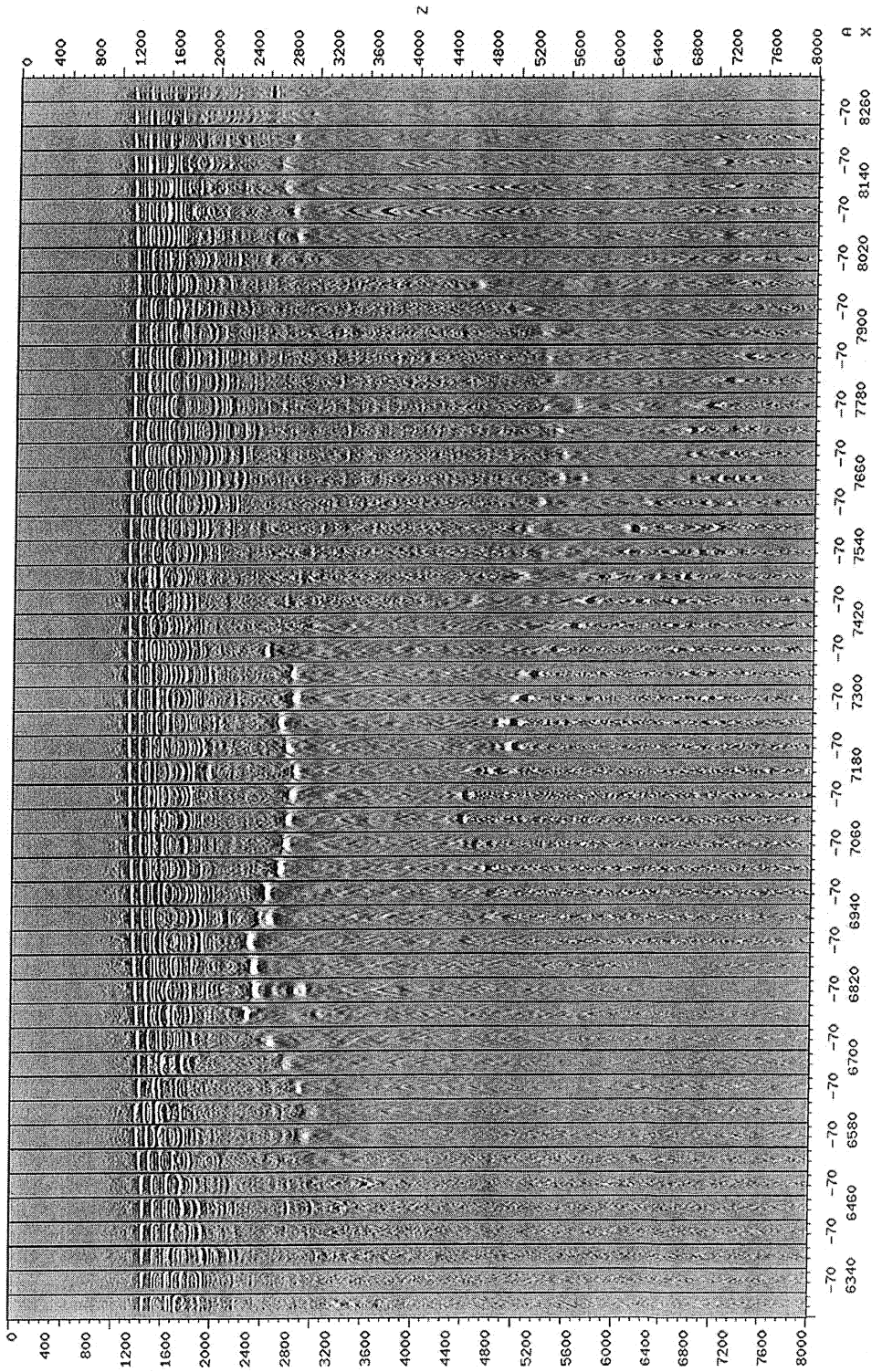

Z
0
400
800
1200
1600
2000
2400
2800
3200
3600
4000
4400
4800
5200
5600
6000
6400
6800
7200
7600
8000
A
X
-70
6340
6460
6580
6700
6820
6940
7060
7180
7300
7420
7540
7660
7780
7900
8020
8140
8260

FIG. 3B

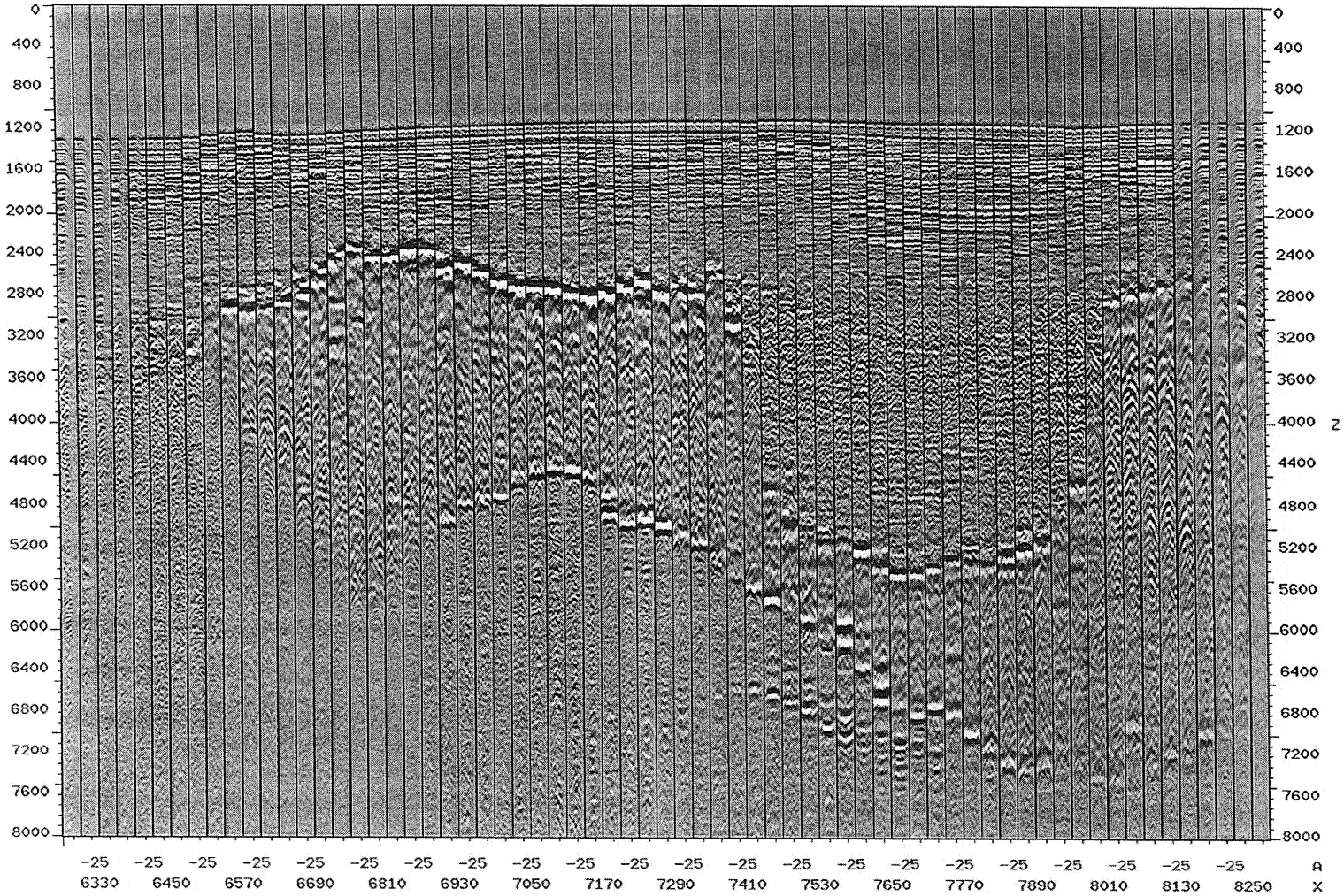

0
400
800
1200
1600
2000
2400
2800
3200
3600
4000
4400
4800
5200
5600
6000
6400
6800
7200
7600
8000
Z
-25 -25 -25 -25 -25 -25 -25 -25 -25 -25 -25 -25 -25 -25 -25 -25 -25 -25 -25 -25 -25
6330 6450 6570 6690 6810 6930 7050 7170 7290 7410 7530 7650 7770 7890 8010 8130 8250
A
X

FIG. 4A

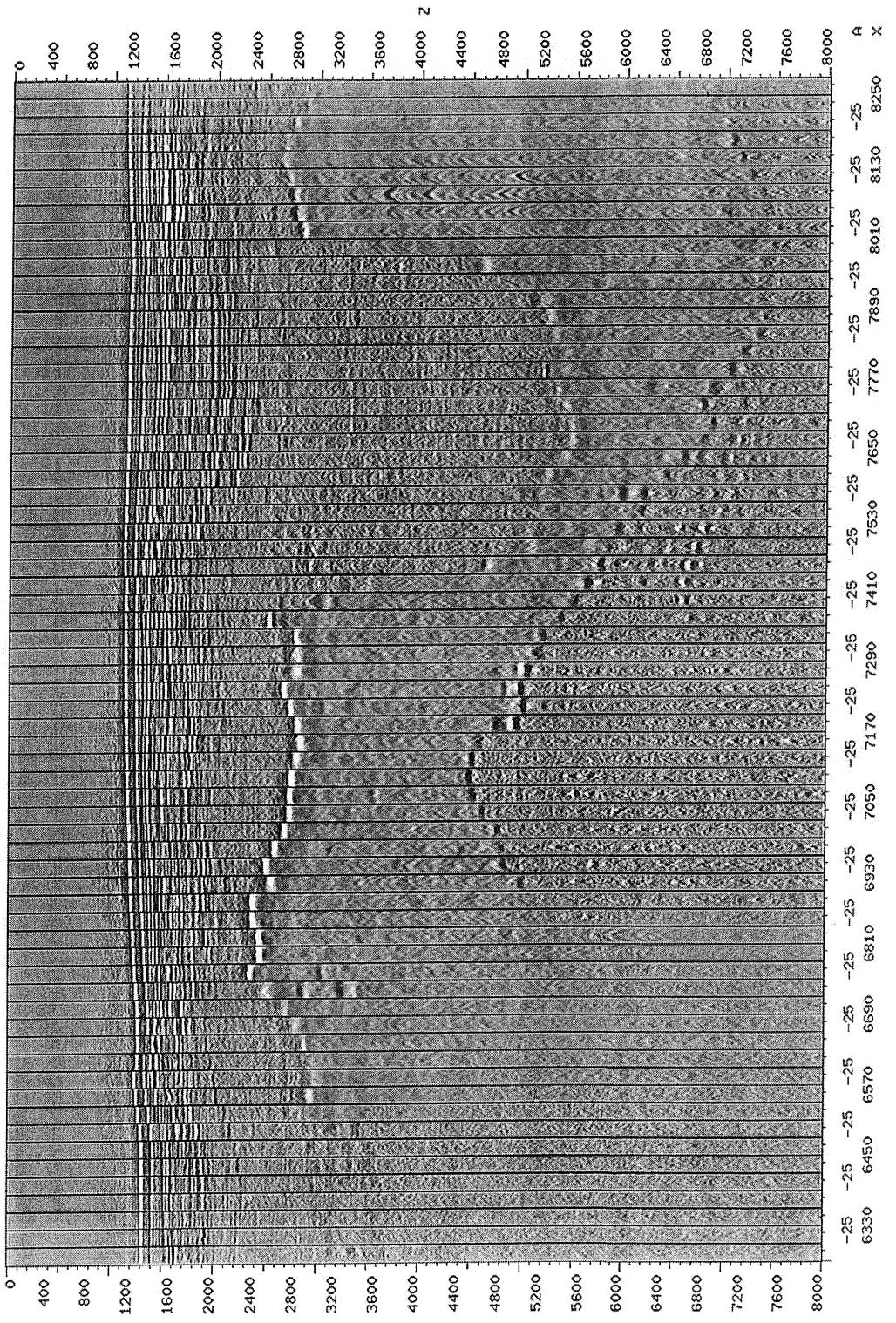

Z
X
0
400
800
1200
1600
2000
2400
2800
3200
3600
4000
4400
4800
5200
5600
6000
6400
6800
7200
7600
8000
-25
6330
6450
6570
6690
6810
6930
7050
7170
7290
7410
7530
7650
7770
7890
8010
8130
8250

FIG. 4B

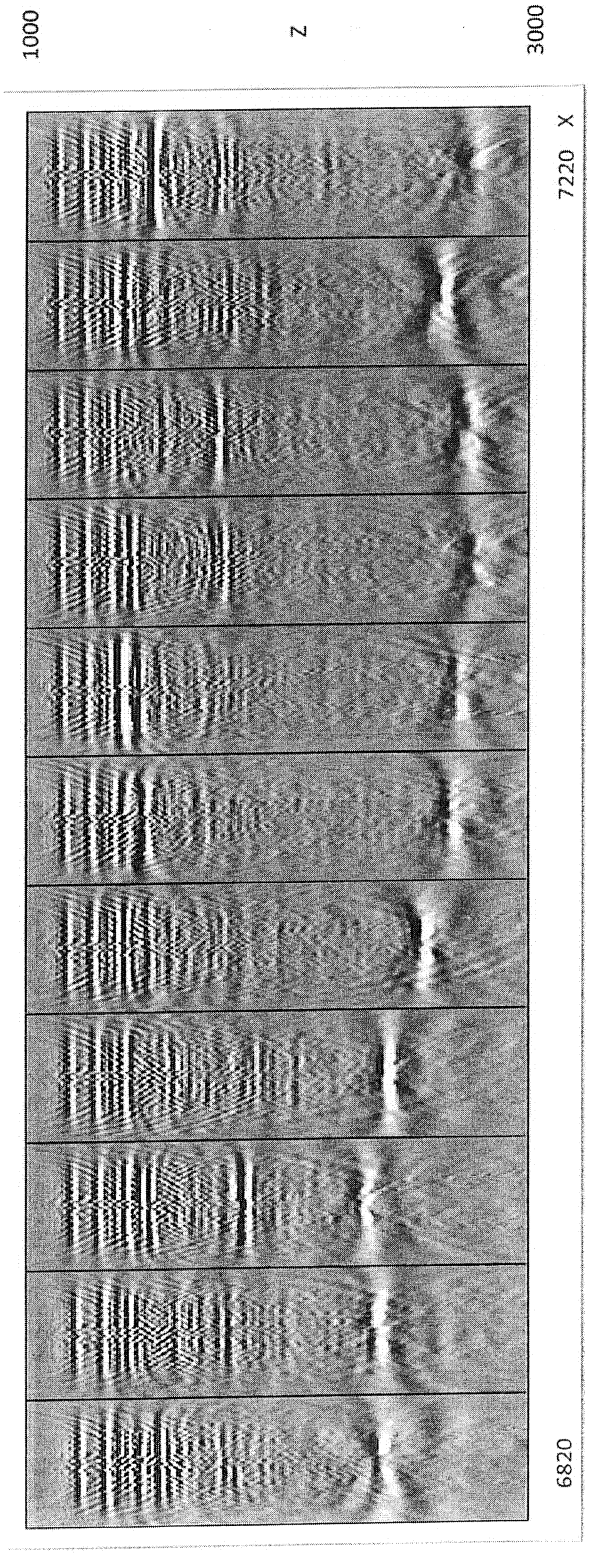


FIG. 5A

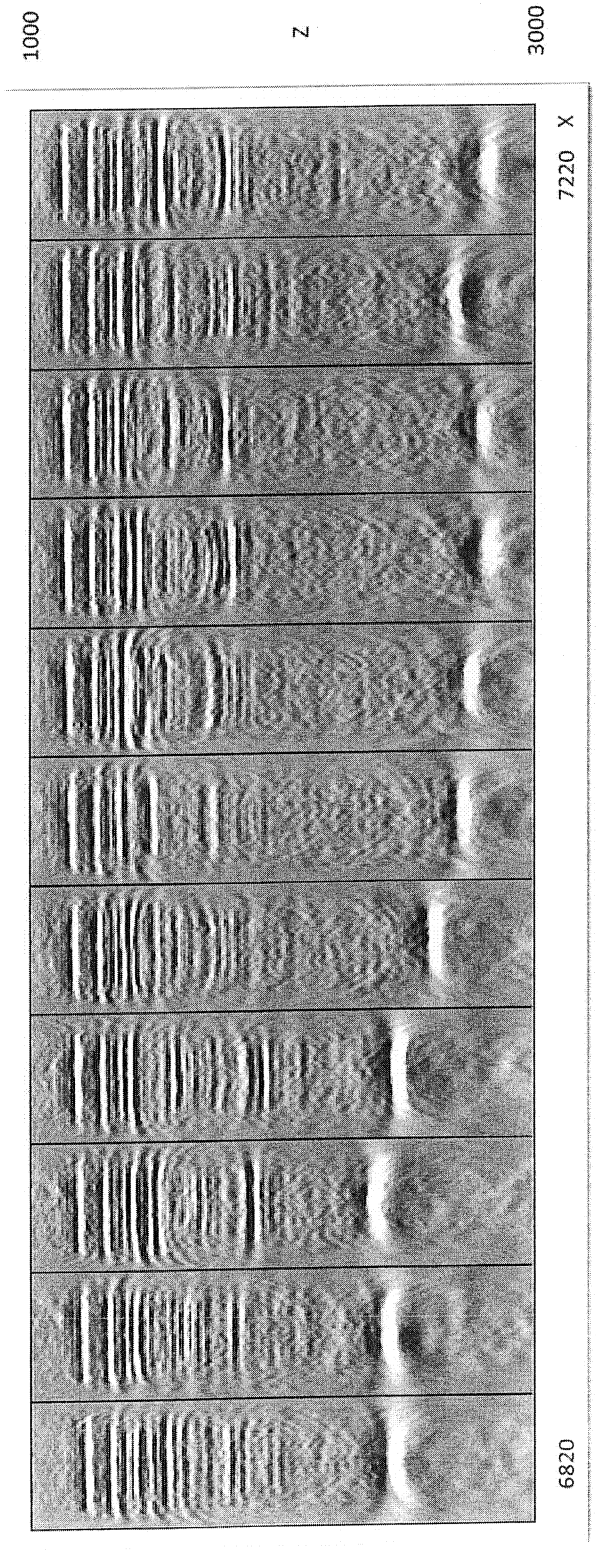


FIG. 5B

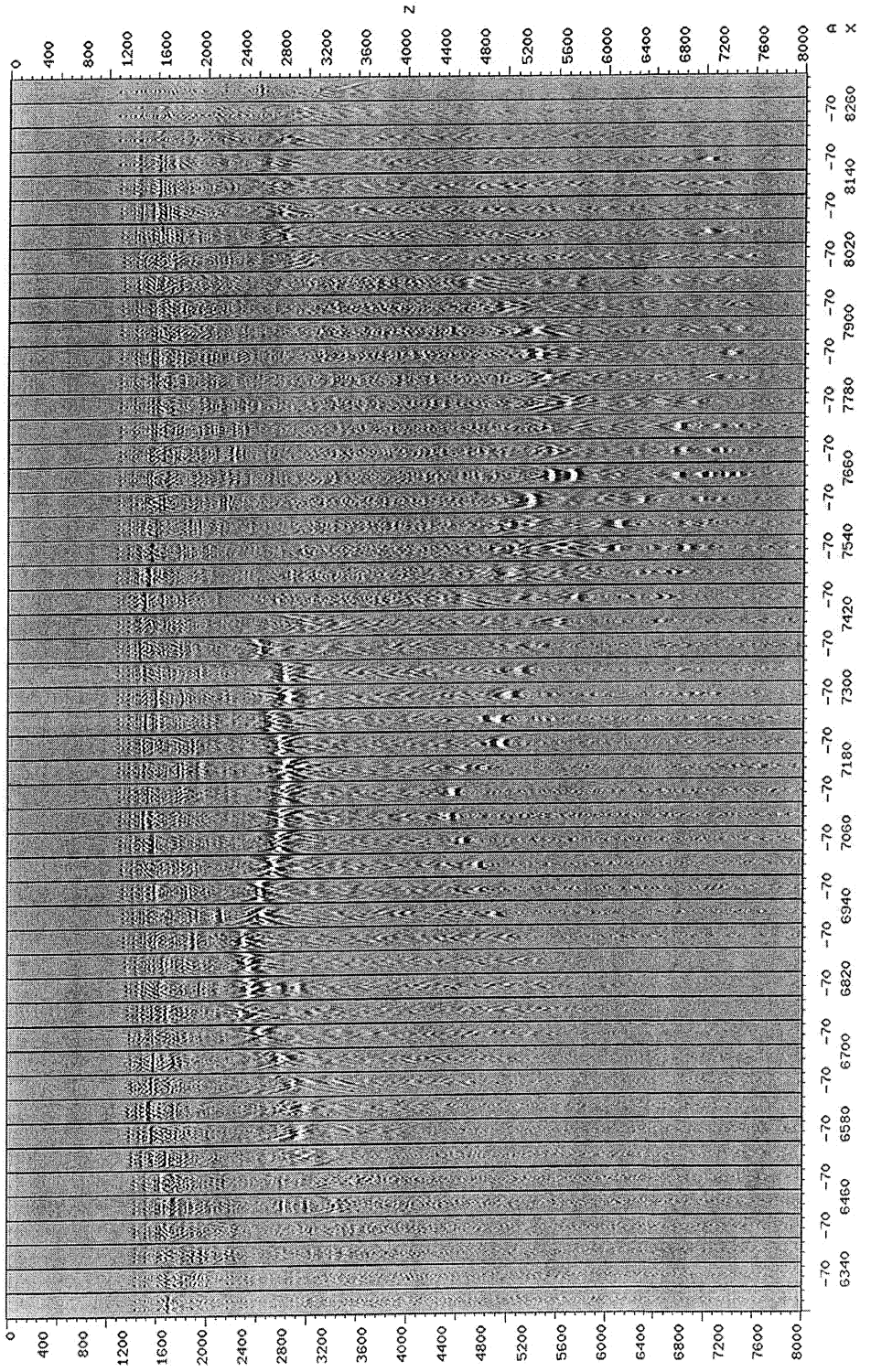

Z
X
0
400
800
1200
1600
2000
2400
2800
3200
3600
4000
4400
4800
5200
5600
6000
6400
6800
7200
7600
8000
6340
6460
6580
6700
6820
6940
7060
7180
7300
7420
7540
7660
7780
7900
8020
8140
8260
-70

FIG. 6A

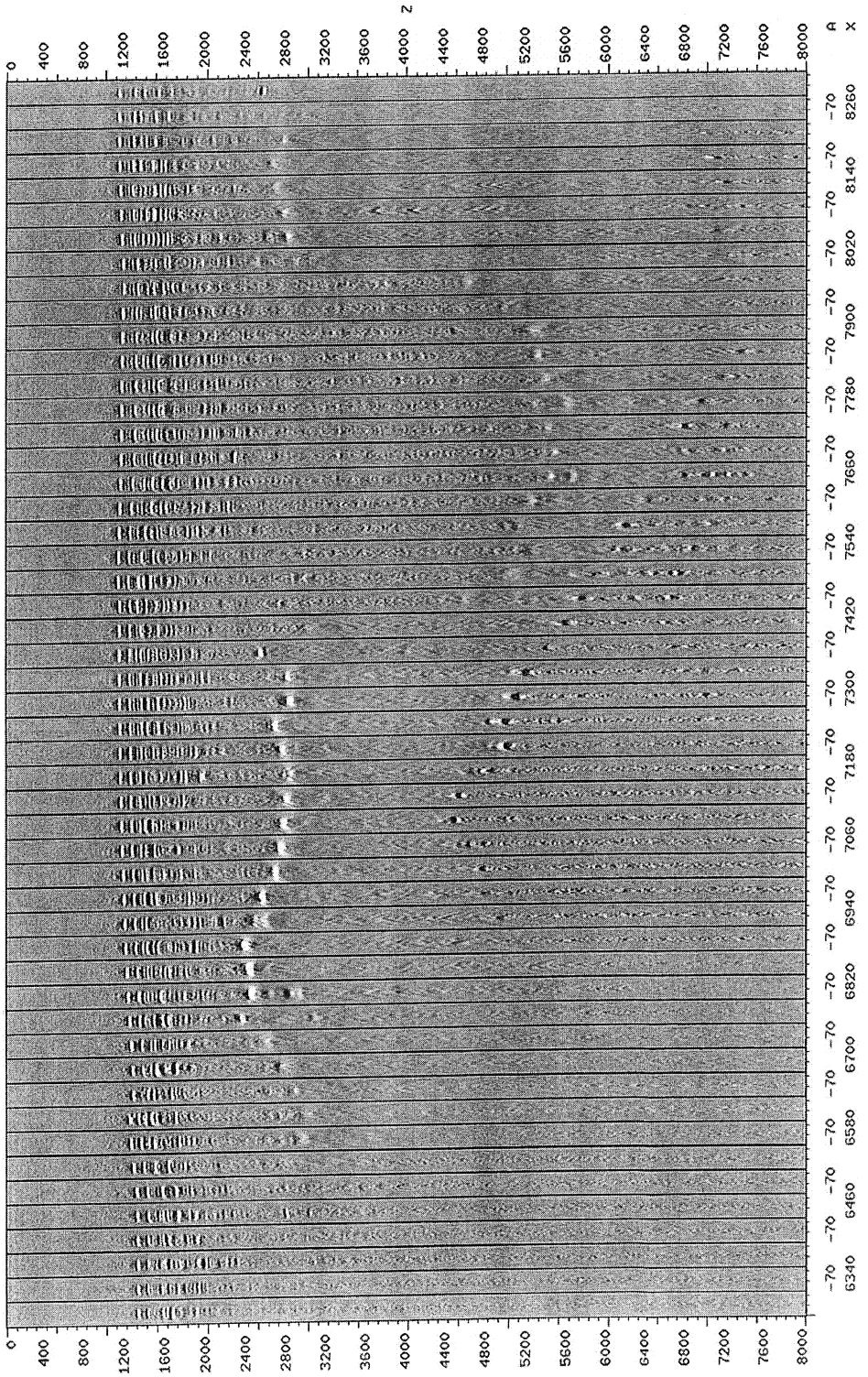

Z
X
0
400
800
1200
1600
2000
2400
2800
3200
3600
4000
4400
4800
5200
5600
6000
6400
6800
7200
7600
8000
6340
6460
6580
6700
6820
6940
7060
7180
7300
7420
7540
7660
7780
7900
8020
8140
8260
-70

FIG. 6B

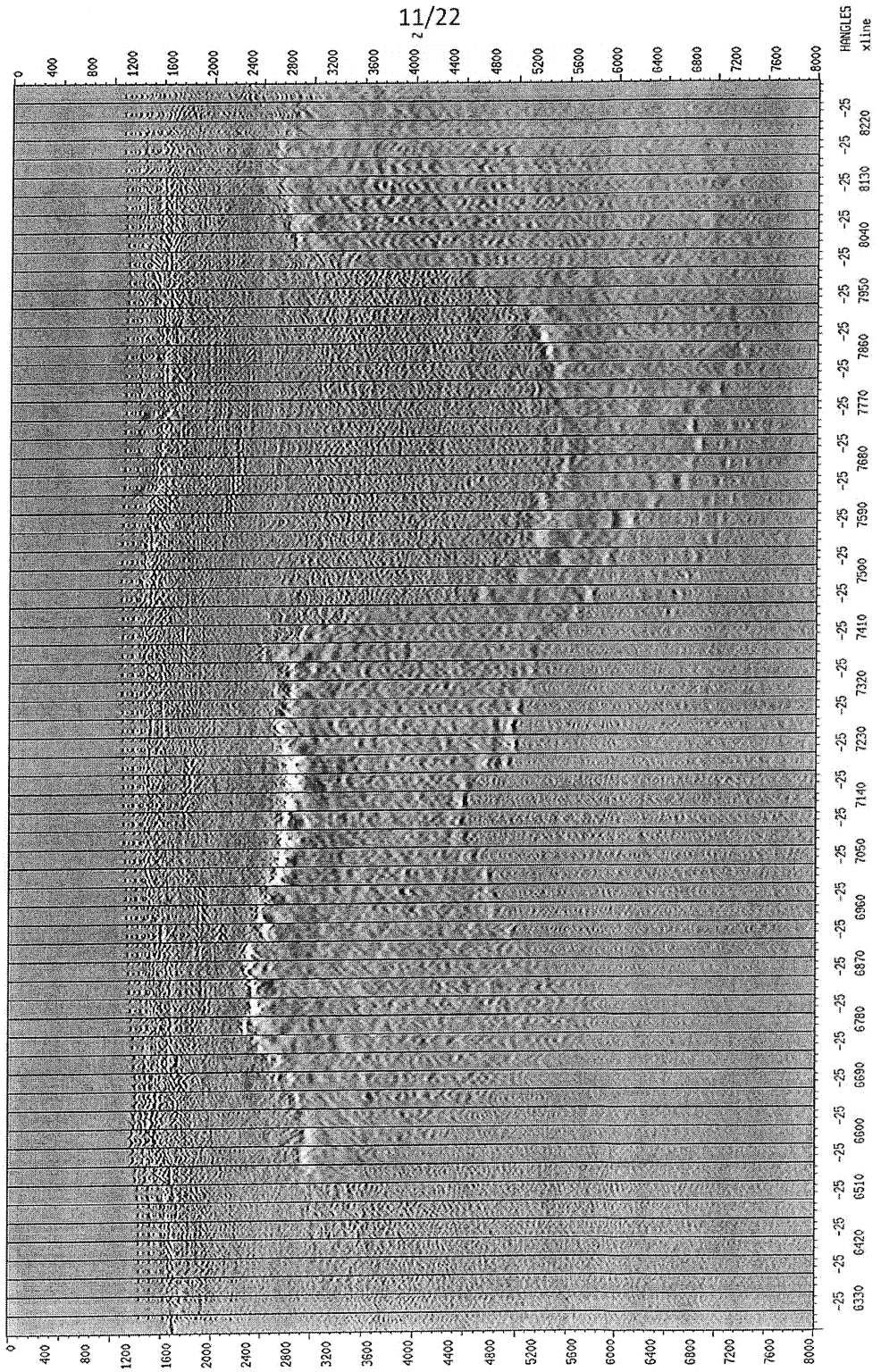

z
0
400
800
1200
1600
2000
2400
2800
3200
3600
4000
4400
4800
5200
5600
6000
6400
6800
7200
7600
8000
HANGLES
xline
-25
6330
6420
6510
6600
6690
6780
6870
6960
7050
7140
7230
7320
7410
7500
7590
7680
7770
7860
7950
8040
8130
8220

FIG. 7A

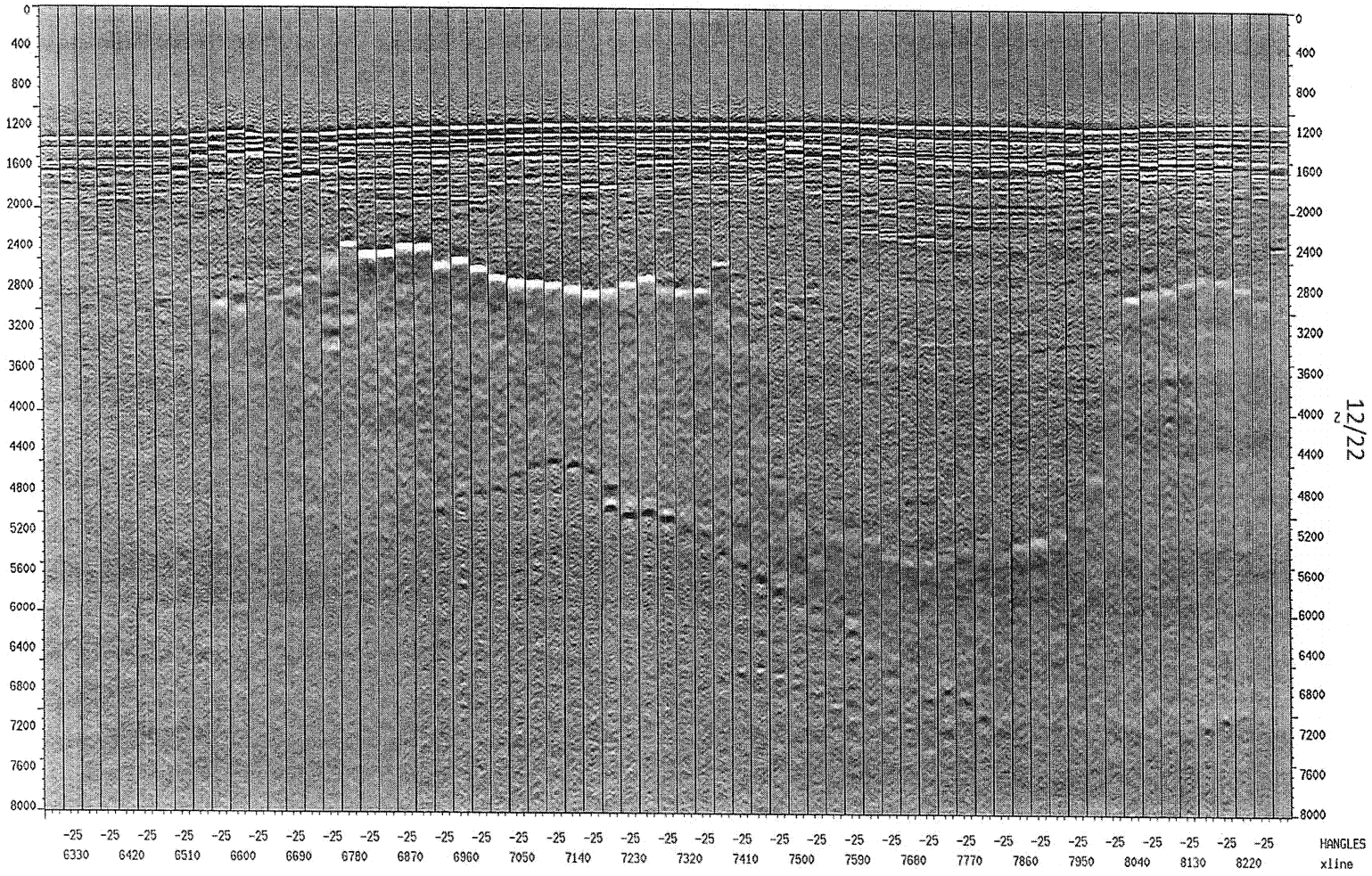

0
400
800
1200
1600
2000
2400
2800
3200
3600
4000
4400
4800
5200
5600
6000
6400
6800
7200
7600
8000
Z
-25 -25 -25 -25 -25 -25 -25 -25 -25 -25 -25 -25 -25 -25 -25 -25 -25 -25 -25 -25 -25 -25 -25 -25 -25 -25 -25 -25 -25 -25 -25 -25
6330 6420 6510 6600 6690 6780 6870 6960 7050 7140 7230 7320 7410 7500 7590 7680 7770 7860 7950 8040 8130 8220
HANGLES
xline

FIG. 7B

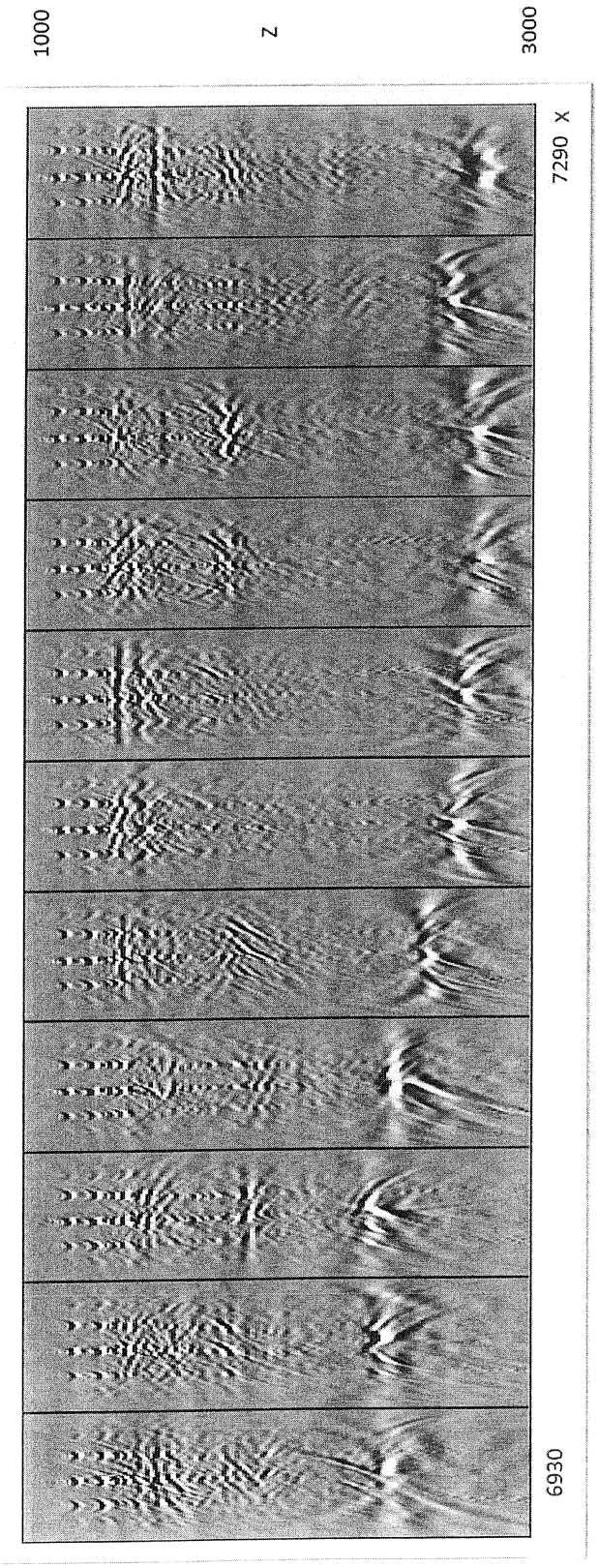


FIG. 8A

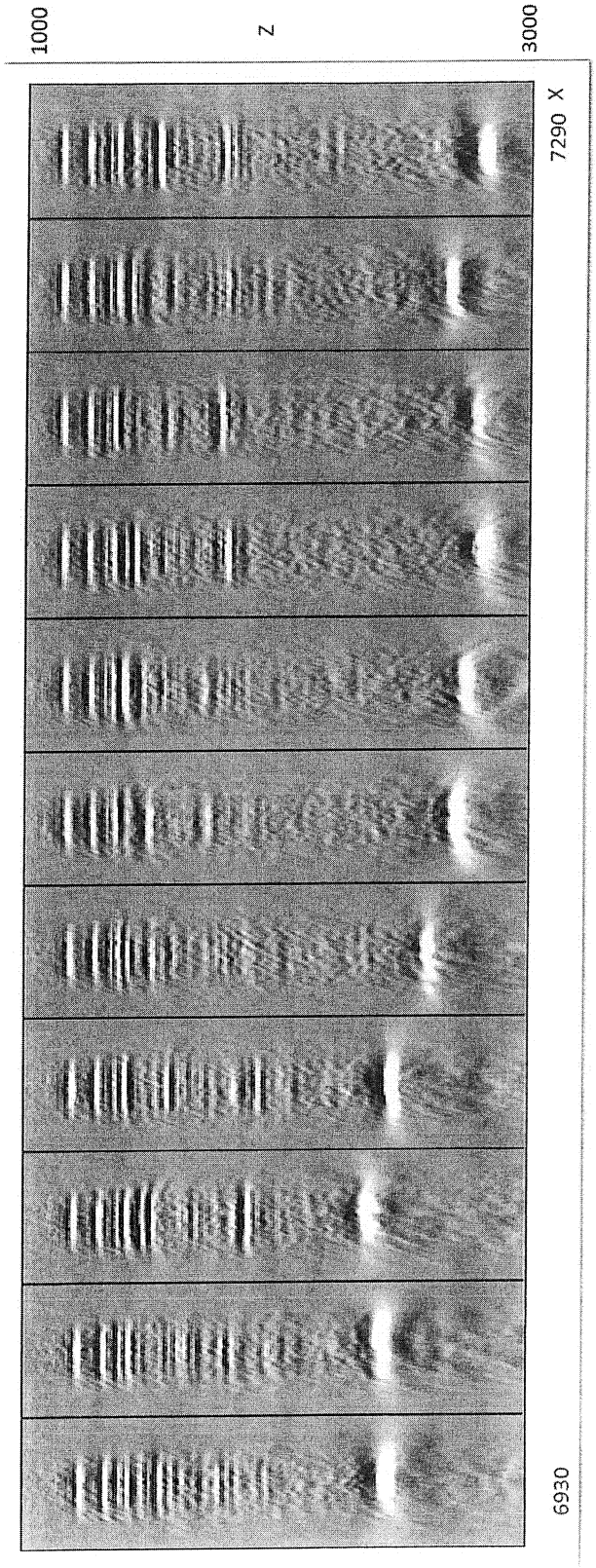


FIG. 8B

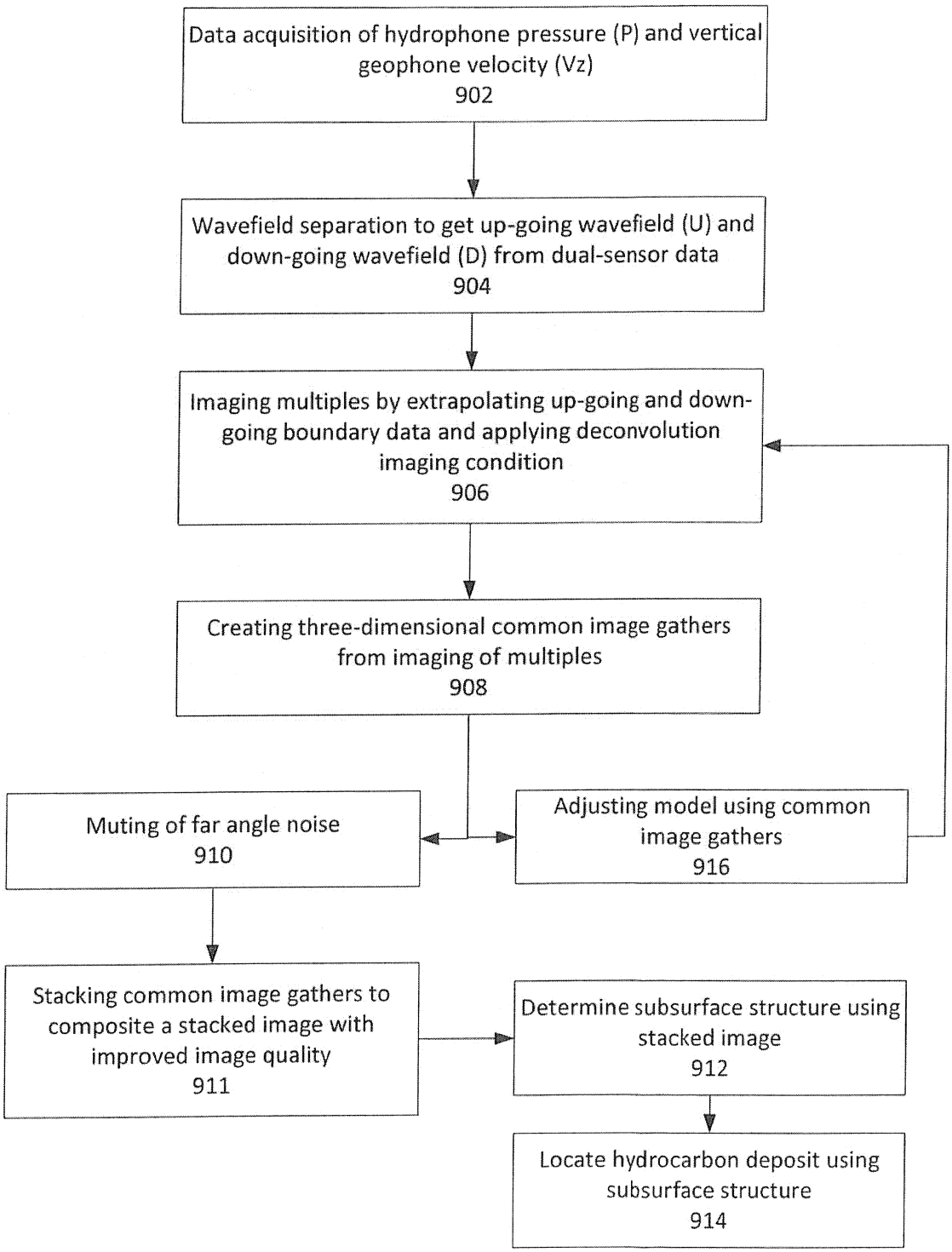

Data acquisition of hydrophone pressure (P) and vertical geophone velocity (Vz)
902
Wavefield separation to get up-going wavefield (U) and down-going wavefield (D) from dual-sensor data
904
Imaging multiples by extrapolating up-going and down-going boundary data and applying deconvolution imaging condition
906
Creating three-dimensional common image gathers from imaging of multiples
908
Muting of far angle noise
910
Adjusting model using common image gathers
916
Stacking common image gathers to composite a stacked image with improved image quality
911
Determine subsurface structure using stacked image
912
Locate hydrocarbon deposit using subsurface structure
914

FIG. 9A

900

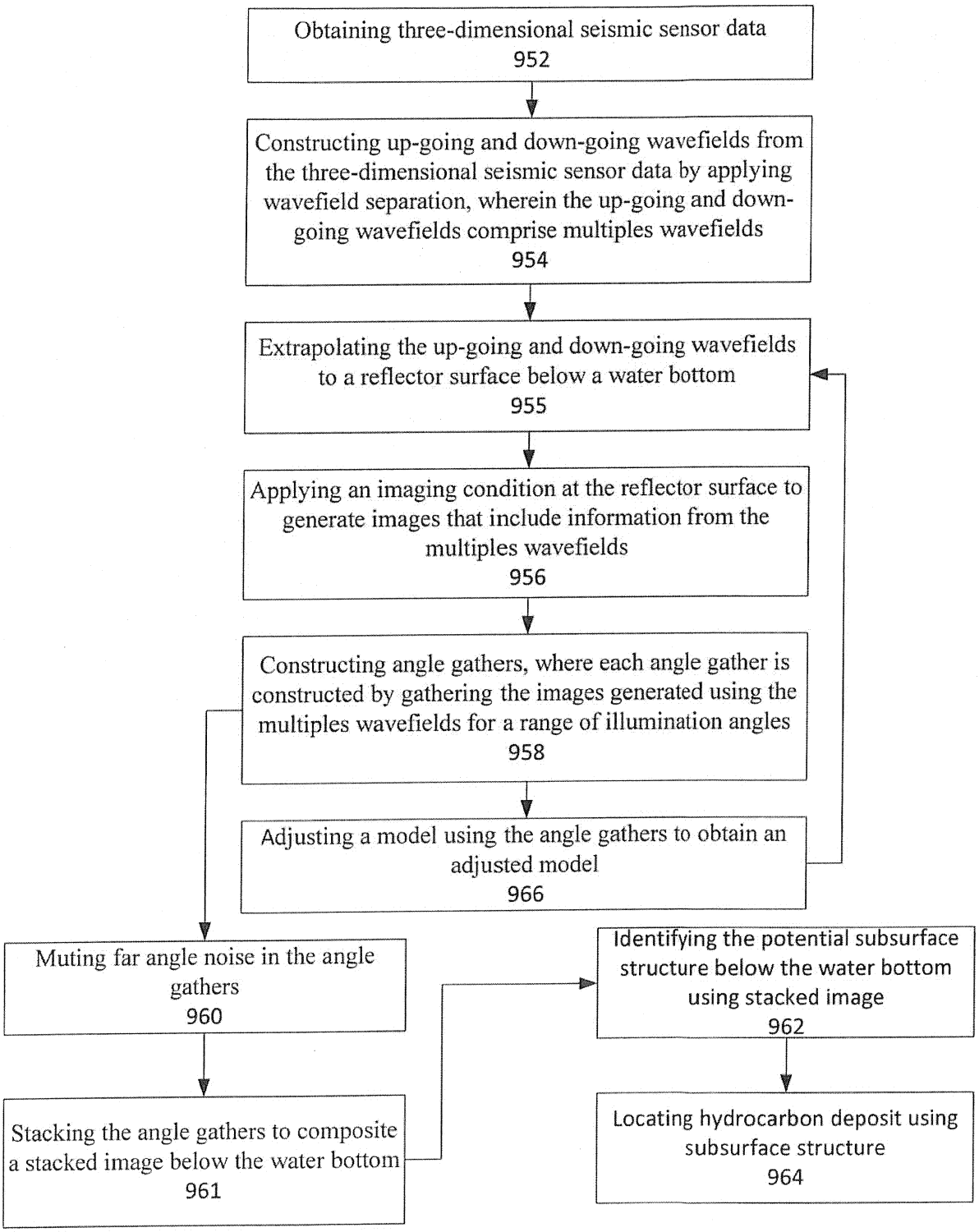

Obtaining three-dimensional seismic sensor data
952
Constructing up-going and down-going wavefields from the three-dimensional seismic sensor data by applying wavefield separation, wherein the up-going and down-going wavefields comprise multiples wavefields
954
Extrapolating the up-going and down-going wavefields to a reflector surface below a water bottom
955
Applying an imaging condition at the reflector surface to generate images that include information from the multiples wavefields
956
Constructing angle gathers, where each angle gather is constructed by gathering the images generated using the multiples wavefields for a range of illumination angles
958
Adjusting a model using the angle gathers to obtain an adjusted model
966
Muting far angle noise in the angle gathers
960
Stacking the angle gathers to composite a stacked image below the water bottom
961
Identifying the potential subsurface structure below the water bottom using stacked image
962
Locating hydrocarbon deposit using subsurface structure
964

FIG. 9B

950

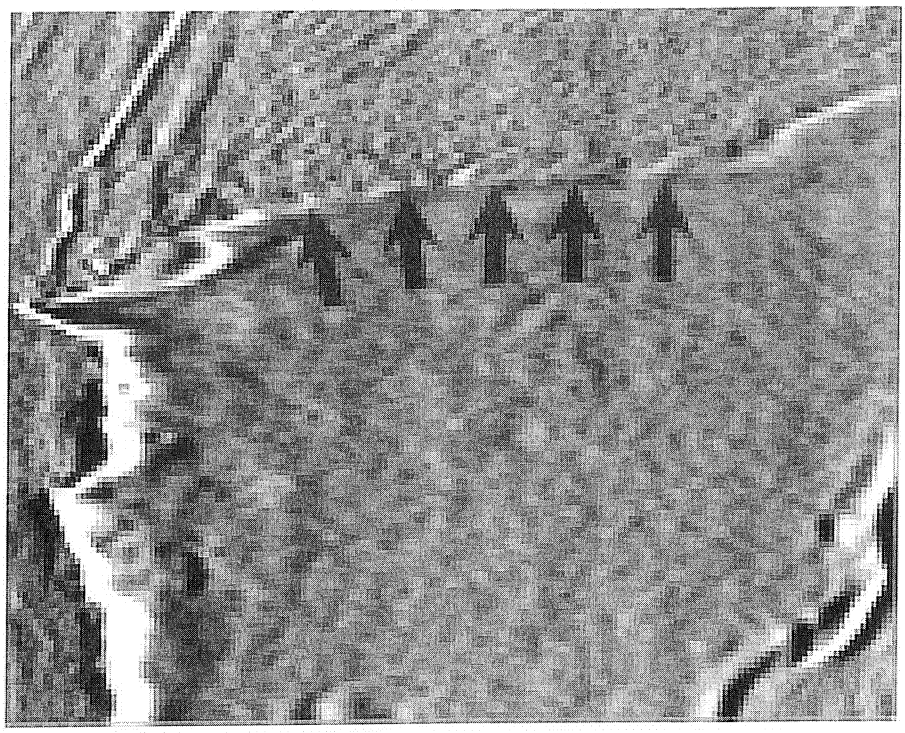


FIG. 10B

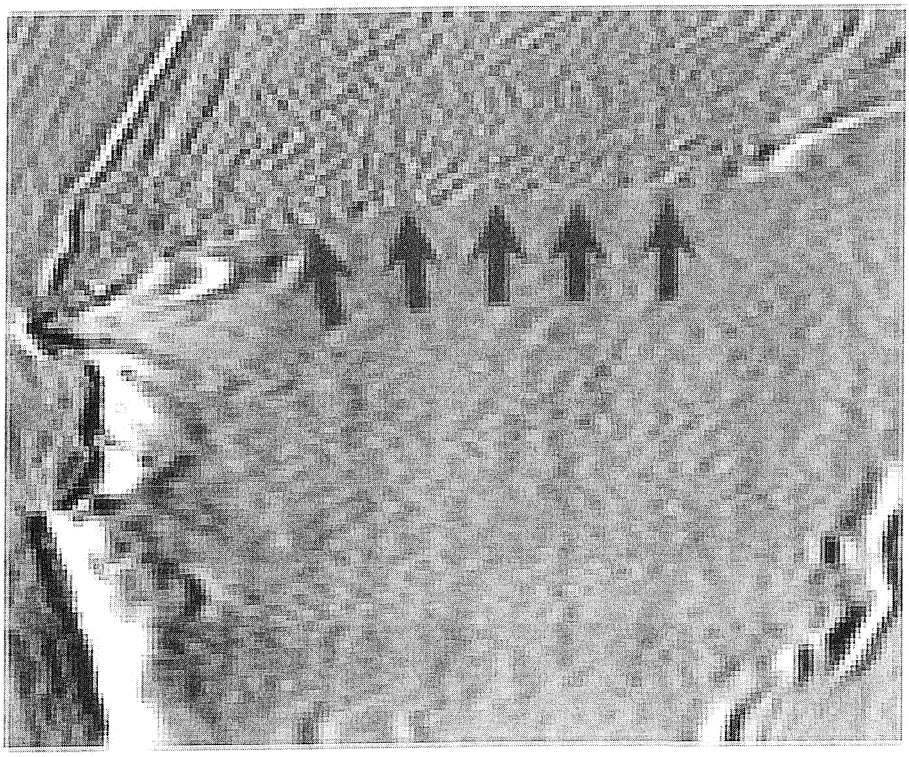


FIG. 10A

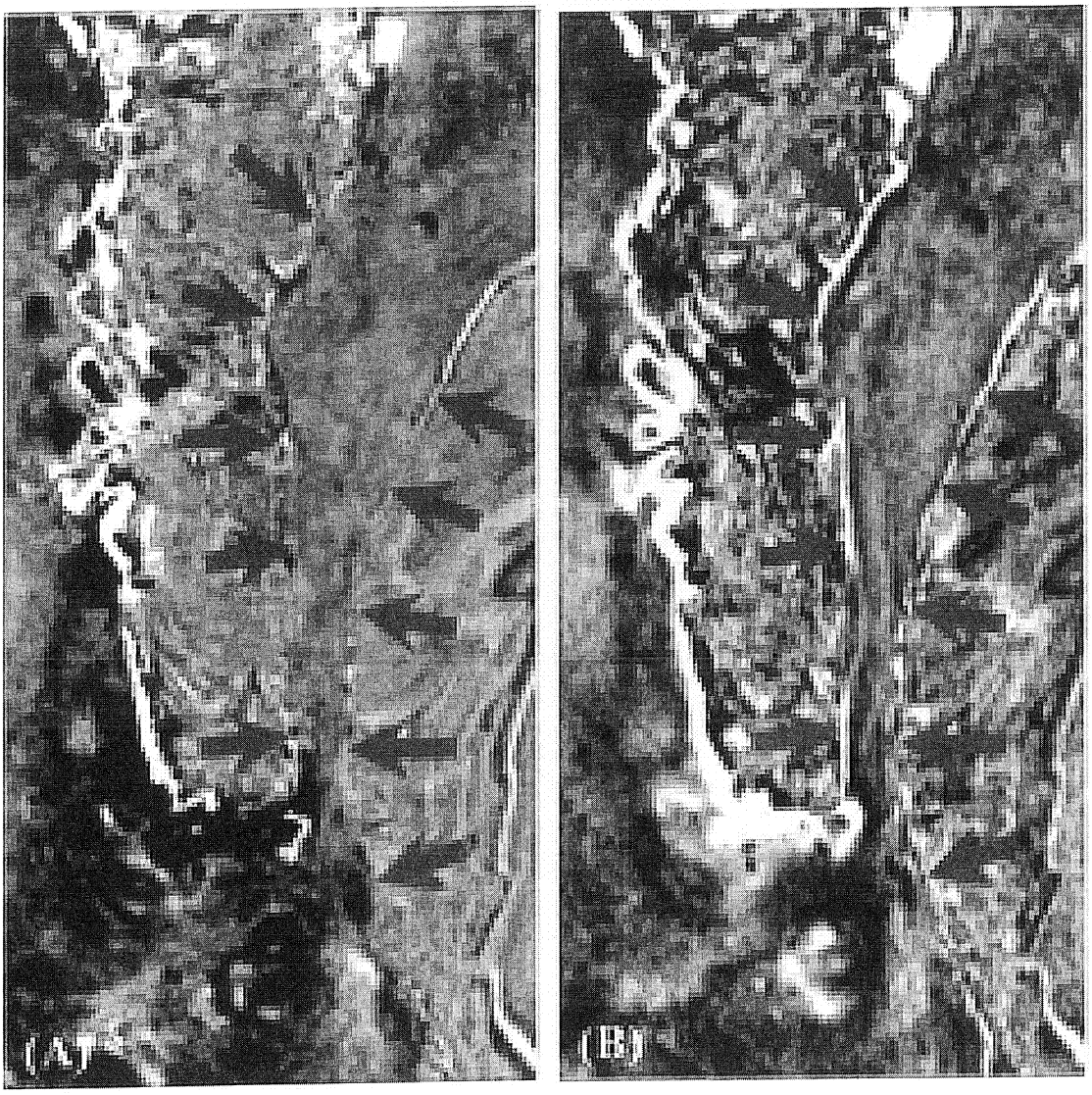


FIG. 11A

FIG. 11B

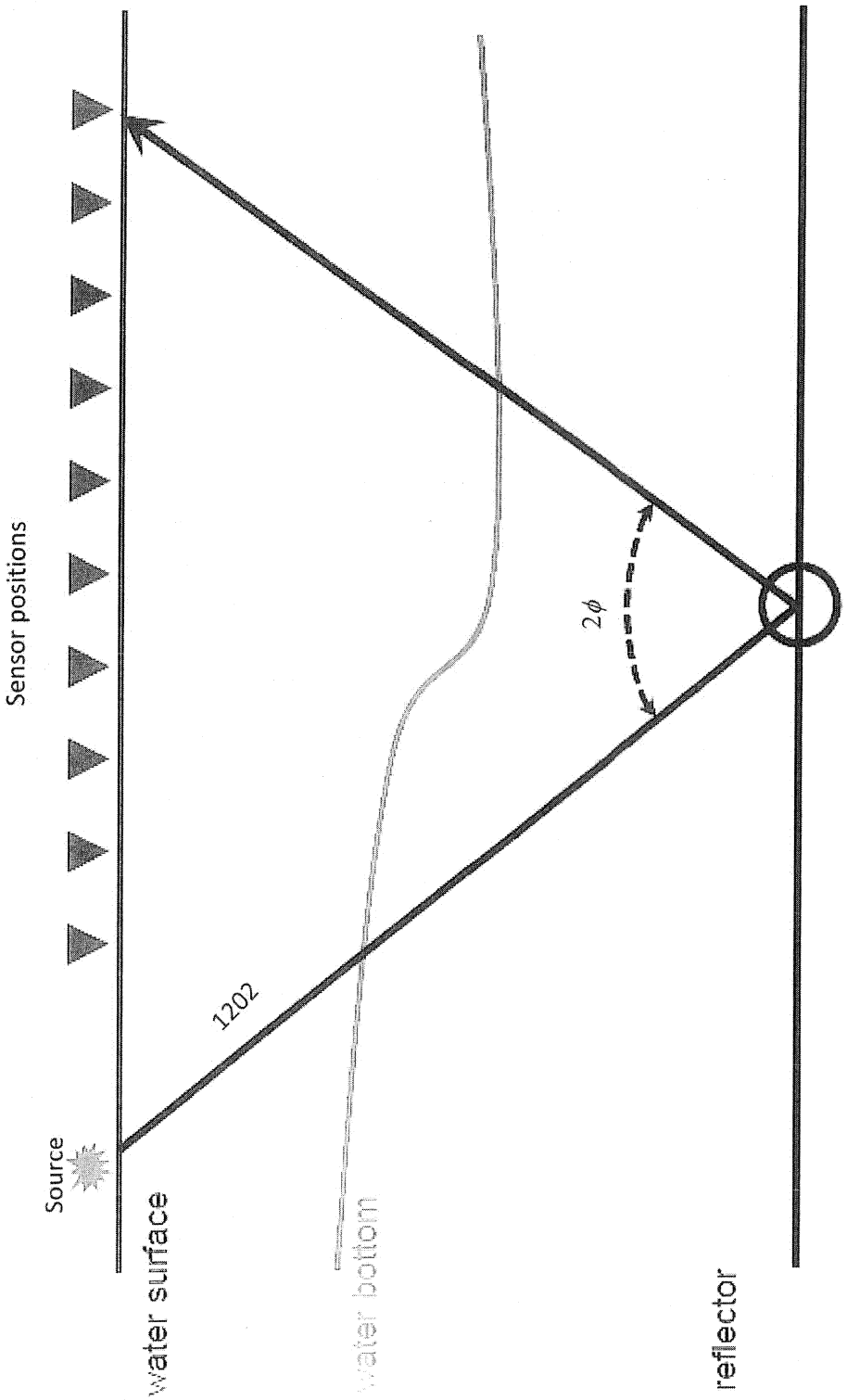

Sensor positions
Source
water surface
1202
water bottom
2ϕ
reflector

FIG. 12

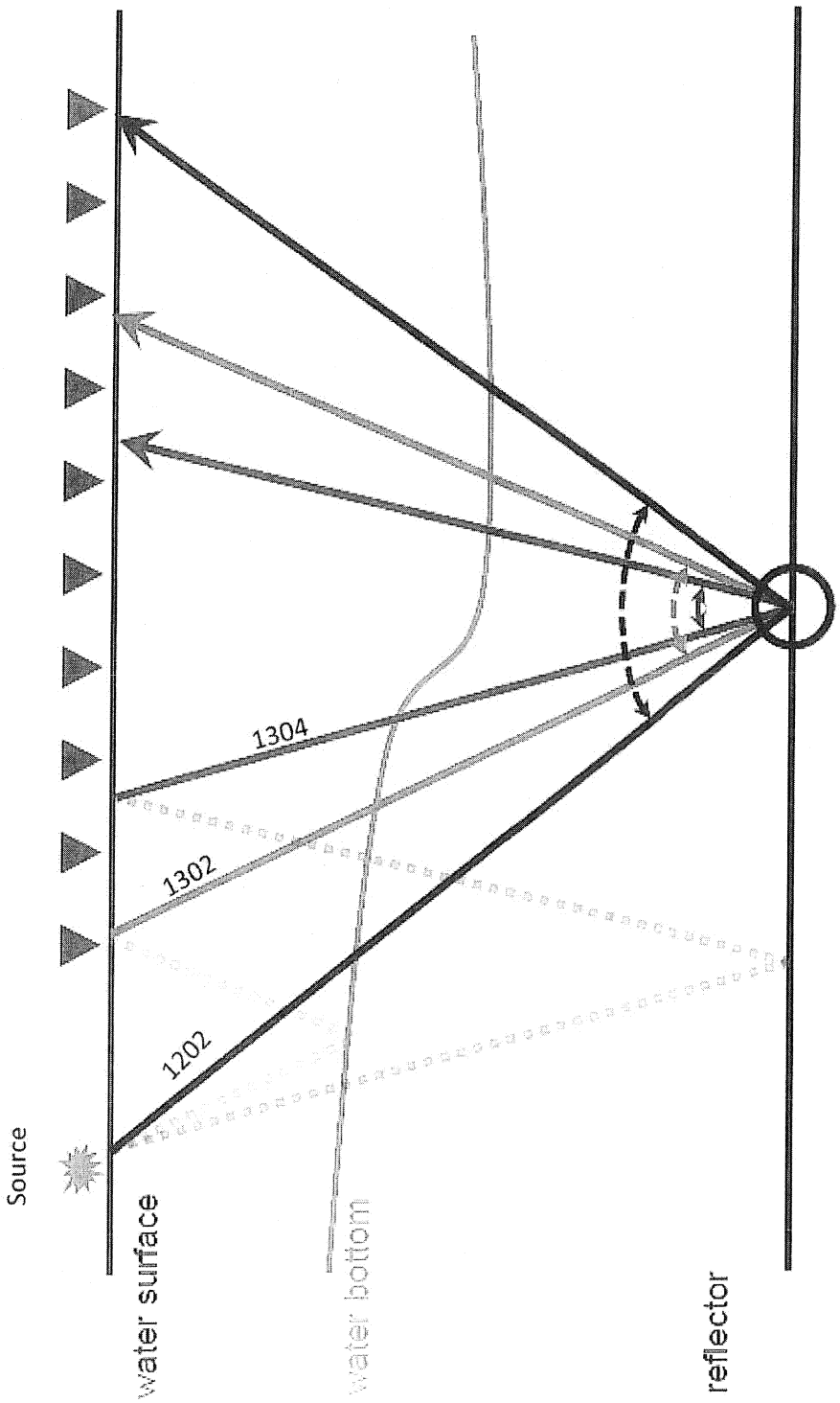

Source
water surface
water bottom
reflector
1202
1302
1304

FIG. 13

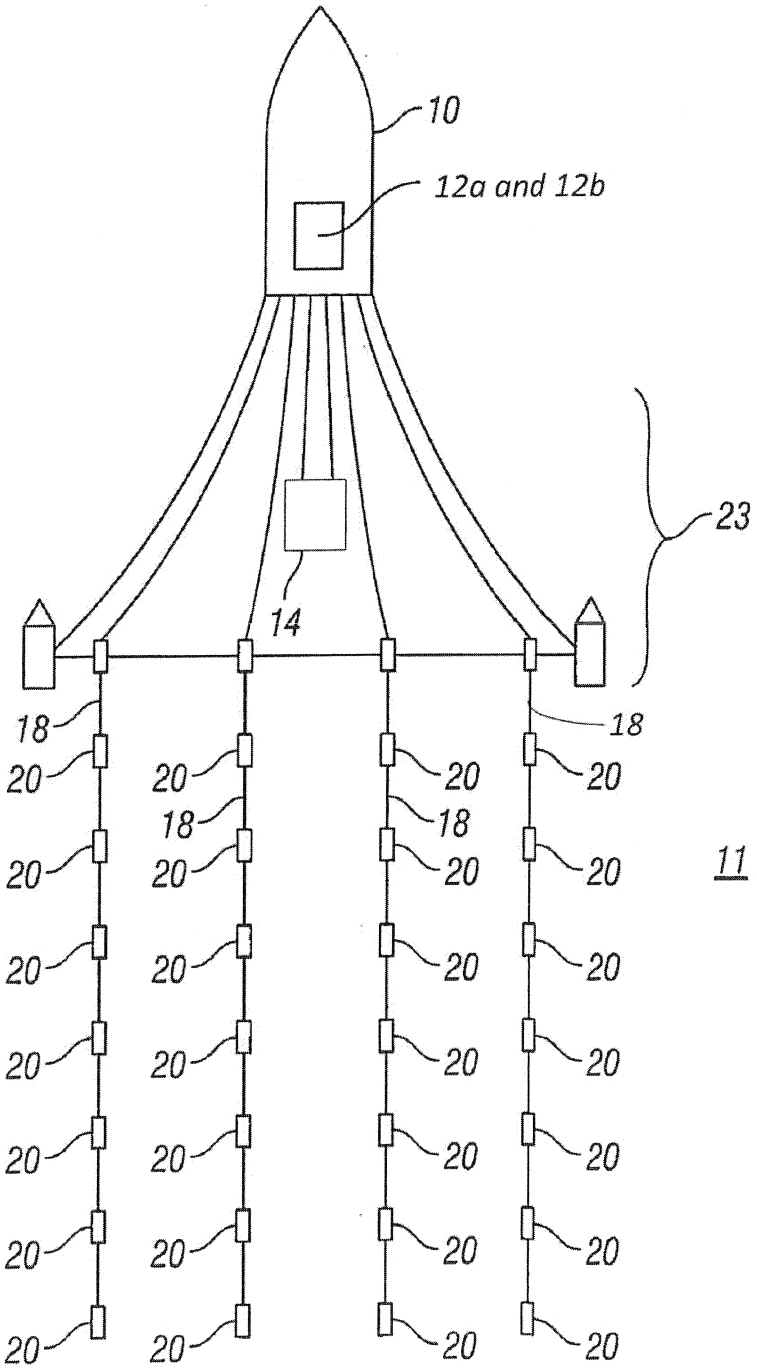


FIG. 14

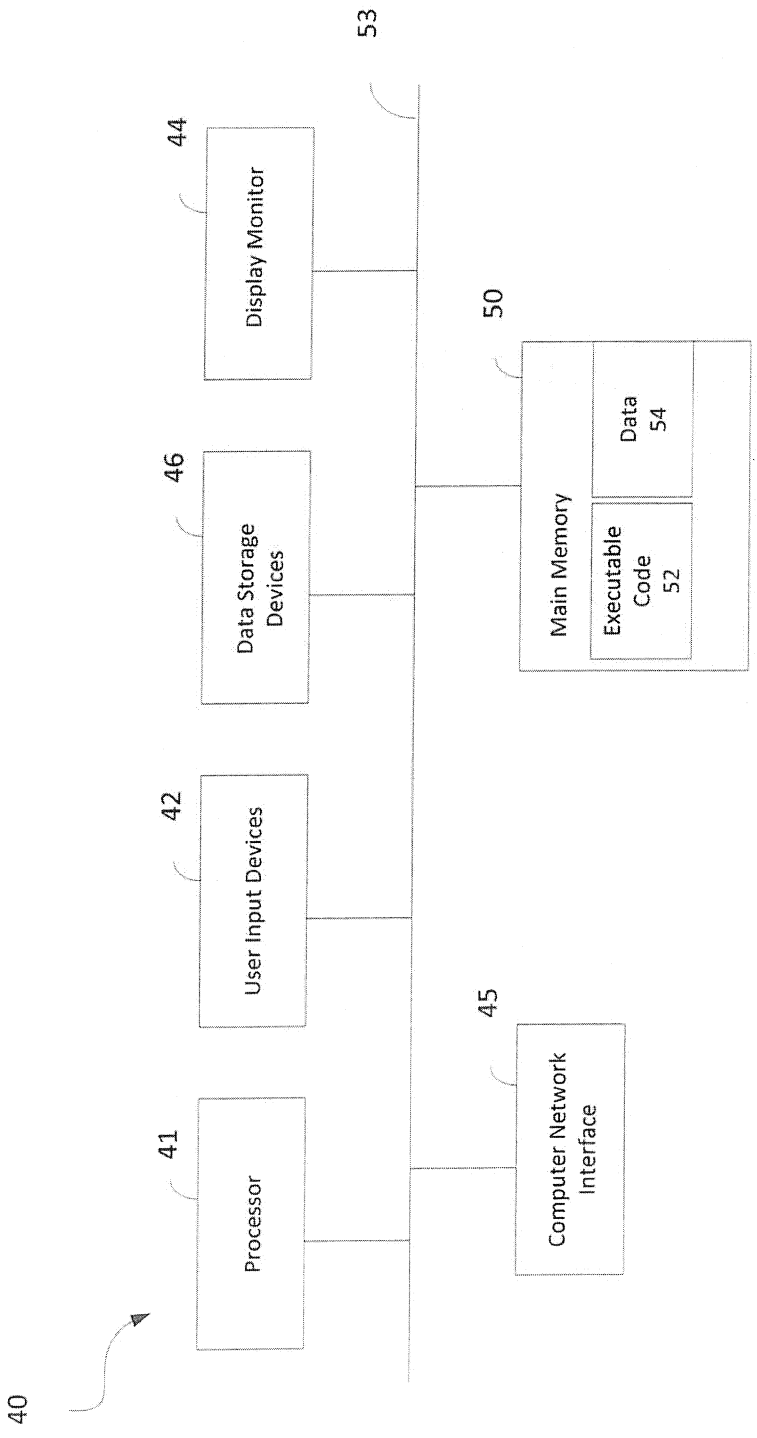

40
41
Processor
42
User Input Devices
45
Computer Network Interface
46
Data Storage Devices
44
Display Monitor
53
50
Main Memory
Executable Code 52
Data 54

FIG. 15